ELSEVIER

Journal of Molecular Catalysis A: Chemical 142 (1999) 85–100

JOURNAL OF MOLECULAR CATALYSIS A: CHEMICAL

Acid-redox properties of titania-supported 12-molybdophosphates for methanol oxidation

S. Damyanova [a], M.L. Cubeiro [b], J.L.G. Fierro [c,*]

[a] *Institute of Catalysis, Bulgarian Academy of Sciences, 1113 Sofia, Bulgaria*
[b] *Facultad de Ciencias, Universidad Central de Venezuela, Apdo. 47102, Caracas, Venezuela*
[c] *Instituto de Catálisis y Petroleoquímica, CSIC, Cantoblanco, 28049 Madrid, Spain*

Received 30 April 1998; accepted 4 August 1998

Abstract

Physicochemical and catalytic properties of titania-supported 12-molybdophosphates have been investigated. The samples were characterized by the *S*(BET) method, Fourier-transform infrared (FTIR) and X-ray photoelectron (XPS) spectroscopies, temperature-programmed desorption (TPD) of ammonia and temperature-programmed reduction (TPR). The effect of temperature pretreatment on the catalytic behaviour of the samples in methanol oxidation was investigated. A significant change of selectivity to the main reaction products: dimethyl ether (DME) and formaldehyde (HCHO), as a function of the acid properties of the catalysts was observed. The highest selectivity to DME at 523 K suggested that the undecomposed molybdophosphoric acid (HPMo) on titania behaves as an acid catalyst. Pretreatment of the samples at higher temperatures (up to 723 K) and replacement of the protons in HPMo by cations (Co and Ni) lead to development of the redox properties (HCHO formation) of the catalyst, due to the suppression of the Brönsted acidity. The IR and XPS results provided clear evidence for the preservation of Keggin unit up to 623 K pretreatment after test reaction. © 1999 Elsevier Science B.V. All rights reserved.

Keywords: 12-Molybdophosphates; Titania; FTIR; TPD; TPR; XPS; Methanol oxidation

1. Introduction

Due to their unique combination of acid-base and redox properties the heteropolyoxometallates have been used successfully as catalysts in their acidic form or in their cationic exchanged or substituted form for acid and redox catalyzed reactions in both homogeneous and heterogeneous media [1,2]. Many of these studies have concentrated on compounds such as $H_3PW_{12}O_{40}$ or $PMo_{12}O_{40}$, which possess a Keggin structure [3–7] in which 12-edge-sharing octahedra of oxygen atoms with a central atom of W or Mo, surround and share atoms with a central tetrahedron. These bulk compounds catalyse many reactions much more effectively than the conventional protonic acids, such as sulfuric and nitric acids. It has been proposed that the high catalytic efficiency of these heteropoly acids is essentially due to specific properties of the heteropoly anion which can be characterized by very weak basicity and great softness, in addi-

* Corresponding author. Fax: +34-1-585-4760; E-mail: jlgfierro@icp.csic.es

1381-1169/99/$ - see front matter © 1999 Elsevier Science B.V. All rights reserved.
PII: S1381-1169(98)00279-9

tion to a large molecular size. When supported on a suitable carrier, they also work as active solid acid catalysts to be comparable, or to exceed, supported phosphoric acid, silica-alumina and acidic zeolites.

An essential drawback of these compounds is their low thermal stability, dehydration of heteropoly acid (HPA) with subsequent destruction of the Keggin's structure and formation of oxide compounds occurs during thermal treatment [8,9]. Accordingly, a number of studies have focused on the thermal stability of heteropoly acids by supporting them on porous substrates [10–18]. It has been reported that silica [10–12] and carbon [13,14] are good carriers of these heteropoly compounds. The stability of silica-supported 12-molybdophosphoric and 12-molybdosilic acids up to 846 K has been shown by Kasztelan et al. [15]. Rocchiccioli-Deltcheff et al. [16] demonstrated that the 12-molybdophosphoric acid (HPMo) destruction occurs at lower temperature for silica-supported HPMo (523 K) than for the unsupported one by formation of a mixture of β- and α-MoO_3 phases. In addition, the transformation into β-MoO_3 begins at 523 K and ends at 623 K [11]. Contrary to that, Fricke and Öhlman [17] have shown that the thermal stability of HPMo decreases when supported on silica; the lower concentration on the support, the lower stability. Cheng and Luthra [18] studying HPMo on alumina have concluded that the decomposition of polyanion occurs as a result of the strong interaction between the support and heteropolyanion, leading to the formation of the aluminium salt.

Taking into account the numerous studies on the thermal stability or catalytic activity of the supported heteropoly compounds it would be of great interest to study the thermal and catalytic behaviours of these compounds when are supported on titania support. Our previous work [19] has shown that the combination of XRD, TDG, IR, Raman and X-ray photoelectron (XPS) spectroscopic techniques can provide information regarding the surface intermediates which are formed upon thermal treatment of titania-supported 12-molybdophosphates. It has been observed that a titania-supported heteropoly anion preserved the Keggin unit up to a higher temperature than that of an unsupported one. Therefore, it is of great interest to investigate the influence of the modifications of the structure and properties of titania-supported heteropoly compounds on their behaviour in catalytic reaction. Methanol oxidation reaction was chosen as a test reaction to characterize the surface properties of the catalysts [20]. Our preliminary results [20] showed that the presence of acidic and basic sites on the surface of these catalysts is required for the partial oxidation of methanol to dimethyl ether and formaldehyde, respectively. In this work, we attempt to investigate in more detail the influence of the physicochemical properties and the structure of the different phases generated upon pretreatments at different temperatures of titania-supported 12-molybdophosphate catalysts on the methanol oxidation reaction.

2. Experimental

2.1. Catalyst preparation

Commercially available (Aldrich, reagent grade) 12-molybdophosphoric acid, abbreviated as HPMo, was used as a starting material. Ni- and Co-salts were prepared from aqueous solutions of the parent HPMo, to which the stoichiometric amounts of Ni- and Co-nitrates (Merck, reagent grade) were added, as described by Tsigdinos [21]. The TiO_2 support was prepared by hydrolysis of $TiCl_4$ followed by dehydration of $Ti(OH)_4$ xerogel at 373 K and then calcination at 773 K. The BET area of the powder sample was 70 m^2 g^{-1} and phase proportion resulted in 85% anatase and 15% rutile. The titania-supported HPMo (denoted as HPMo/T) and its Co and Ni salts (denoted as CoPMo/T and NiPMo/T, respectively) were prepared by conventional wetness impregnation of TiO_2

powder with aqueous solutions of purified HPMo and its corresponding salts, respectively. The impregnates were then dried at 343 K for 4 h. For characterization studies the samples were heated in air at different temperatures while keeping each temperature for 2 h. Subsequently, they were cooled to room temperature and stored in a dessicator. The spent catalysts were collected in isoctane in order to prevent any further contact with air prior to analysis.

2.2. Techniques and procedures

2.2.1. Chemical analysis

The elemental analysis of catalyst constituents (Mo, P, and Ni or Co) was determined by atomic absorption spectrophotometry using a Perkin Elmer 3030 instrument. The solid samples were first acid digested in a microwave oven for 2 h, and then aliquots of solution were diluted to 50 cm^3 using deionized water (m-Rho quality). The chemical analysis data of the samples is listed in Table 1.

2.2.2. BET area

Specific area of the catalysts was computed according to the BET method from the nitrogen adsorption isotherms obtained at 77 K, taking a value of 0.162 nm^2 for the cross-section of the adsorbed N_2 molecule at that temperature. The nitrogen adsorption isotherms were measured in an automatic Micromeritics ASAP 2000 apparatus, selecting only the range of relative pressures $0.05 < P/P_o < 0.30$ for BET calculation. BET areas of catalysts are summarized in Table 1.

Table 1
Chemical analysis[a] and S_{BET} of the samples

Sample	Mo/Ti	Ni(Co)/Ti	P/Ti	S_{BET} ($m^2\ g^{-1}$)
HPMo/T	0.282	–	0.002	52
NiPMo/T	0.296	0.014	0.003	57
CoPMo/T	0.291	0.014	0.003	63
TiO_2	–	–	–	70

[a]Atomic ratios.

2.2.3. Fourier-transform IR spectroscopy (FTIR)

Lattice vibrations and the IR spectra of chemisorbed molecular probes were recorded on an FTIR Nicolet 5 ZDX spectrophotometer working at a resolution of 4 cm^{-1} and averaged over 100 scans. The framework vibration spectra were recorded in the region 1200–600 cm^{-1} from self-supporting wafers prepared by pelleting the samples 1:100 diluted in KBr. The vibration spectra of chemisorbed pyridine were recorded in the region 1700–1300 cm^{-1}. A special IR cell fitted with greaseless stopcocks and KBr windows was used for this purpose. Self-supporting wafers of the catalysts were outgassed at 10^{-4} Torr (1 Torr = 133.33 Pa) at 523, 623 and 723 K for 1 h. After cooling to room temperature, the samples were exposed to ca. 1.5 Torr pyridine and the physically adsorbed fraction removed by outgassing at 393 K for 1 h before the spectra were recorded. The net spectrum of adsorbed pyridine was obtained by calculating the difference between the total and background spectra.

2.2.4. Temperature-programmed desorption (TPD) of ammonia

TPD patterns of chemisorbed ammonia were recorded with a quadrupole mass filter (Balzers QMS 100) connected on-line with a microreactor. The samples (ca. 0.50 g) were placed in a glass reactor and heated at a rate of 10 K min^{-1} in an Ar flow 100 $cm^3\ min^{-1}$ for 2 h, and then cooled to room temperature under the same atmosphere. Many products were desorbed during catalyst pretreatment. The principal molecules (H_2O, CO, O_2, and CO_2) were followed by recording the masses m/z of 18, 28, 32 and 44. Other m/z masses were also recorded in order to monitor destruction of the NH_3 molecule (m/z of 16, 28, 44 and 46 for NH_3, N_2, N_2O and NO_2 molecules, respectively). A flow of 900 ppm NH_3 in Ar was passed over the samples at 313 K until all the masses reached a constant level. Then, the physically adsorbed ammonia was desorbed in a flow of pure Ar and

subsequently the TPD profile was recorded upon heating the sample at a rate of 10 K min^{-1} up to 843 K.

2.2.5. X-ray photoelectron spectroscopy (XPS)

XP spectra were acquired with a VG ESCALAB 200R spectrometer equipped with a hemispherical electron analyzer and Mg Kα ($h\nu = 1253.6$ eV, 1 eV $= 1.6302 \times 10^{-19}$ J) X-ray source. The powder samples were pressed into small Inox cylinders and then mounted on a heater placed in a pretreatment chamber. Prior to being moved into the analysis chamber the fresh samples were evacuated in the pretreatment chamber of the instrument from 523 to 723 K for 2 h, while the used samples were evacuated at 333 K. The residual pressure in the ion-pumped analysis chamber was maintained below 5×10^{-9} Torr during data acquisition. The intensities of Mo3d, Co2p, Ni2p, P2p and $Ti2p_{3/2}$ peaks were estimated by calculating the integral of each peak after smoothing and subtraction of the 'S-shaped' background and fitting the experimental curve to a combination of Gaussian and Lorentzian lines of variable proportion. The binding energies (BE) were referenced to the C1s peak at 284.9 eV giving BE values with an accuracy of ± 0.1 eV.

2.2.6. Temperature-programmed reduction (TPR)

TPR experiments were recorded on a Micromeritics instrument model TPR/TPD 2900 fitted with a thermo conductivity detector (TCD) and controlled by a computer. The samples (0.025 g) were pretreated at 423 K in a He stream for 1 h in order to remove surface contaminants. After cooling to room temperature, a flow of 10% H_2 in Ar was passed across the samples and the temperature increased at a rate of 10 K min^{-1} up to 873 K while the TCD signal was recorded.

2.3. Activity measurements

Catalytic experiments were performed in a continuous flow system provided by a stainless steel tubular reactor (6.2 mm i.d.) using 0.05 g of catalyst held between two layers of quartz wool. A CH_3OH:O_2:He = 5:10:85 (molar ratio) mixture was fed into the reactor at a rate of 100 cm^3 min^{-1} at atmospheric pressure. Liquid methanol was fed by means of a liquid pump (Becton-Dickinson) and vaporized in a preheater prior to the reactor inlet. The products were analyzed by an on-line gas chromatograph (GC, Varian 3400 CX) provided with a TCD and a Porapack N packed column. In order to avoid condensation of the reactor effluents, the outlet of the reactor-GC inlet was heated to 393 K. Blank runs were conducted with an empty reactor without any detectable conversion. Pretreatment of the samples was done at the corresponding calcination temperature for 1 h in an O_2:He = 10:90 (molar ratio) mixture prior to each run. Catalytic runs were obtained for 12–15 h, beginning 10 min after methanol was injected through the reactor, on each sample at 483 and 503 K, always in increasing order of temperature, to obtain conversion and selectivity data.

3. Results

3.1. Framework vibrations

The FTIR spectra of HPMo/T and Co(Ni)PMo/T catalysts before and after on-stream reaction are shown in Figs. 1 and 2, respectively. For comparative purposes, the infrared spectrum of fresh bulk HPMo is also included in Fig. 1. The IR spectra of bulk HPMo (Fig. 1A) shows the bands at 1065, 962, 873 and 787 cm^{-1} assigned to stretching vibrations ν_{as}(P–O_d), ν_{as}(Mo–O_t), ν_{as}(Mo–O_b–Mo) and ν_{as}(Mo–O_c–Mo), respectively, characterizing the Keggin unit [22]. As for the titania-supported HPMo and Co(Ni)PMo catalysts there are strong framework vibration bands of the TiO_2 carrier below 900 cm^{-1} which overshadow that coming from the Keggin structure, no further attention will be paid to this region for the supported HPMo and its salts. Consequently, the Keggin unit on titania can be char-

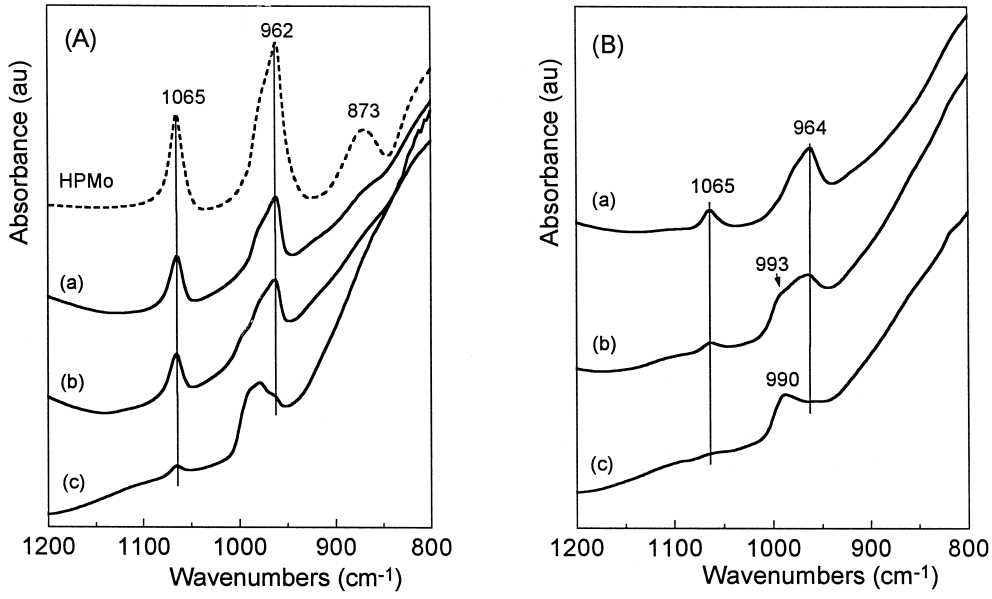

Fig. 1. IR spectra of fresh (A) and used (B) TiO_2-supported HPMo catalysts subjected to different pretreatment temperatures: (a) 523 K, (b) 623 K, and (c) 723 K.

acterized only by its two highest frequencies (1065 and 962 cm^{-1}), which are identical to the bulk HPMo up to 523 K (Figs. 1 and 2). Upon heating at 623 K, only small changes in the spectrum of HPMo/T sample are observed as a consequence of a partial degradation of the heteropoly anion [19], a small band of MoO_3 at 993 cm^{-1} on the higher wavenumber side of the stretching vibration $\nu_{as}(Mo–O_t)$ begins to appear. However, a significant changes are observed in the spectrum of the sample heated at 723 K. The HPMo is decomposed into molybdenum oxide phases (α-MoO_3 and β-MoO_3 [19]) with preserved Keggin unit, as revealed by the appearance of a visible band at 990 cm^{-1} and the simultaneous decrease of the main bands at 1065 and 962 cm^{-1}.

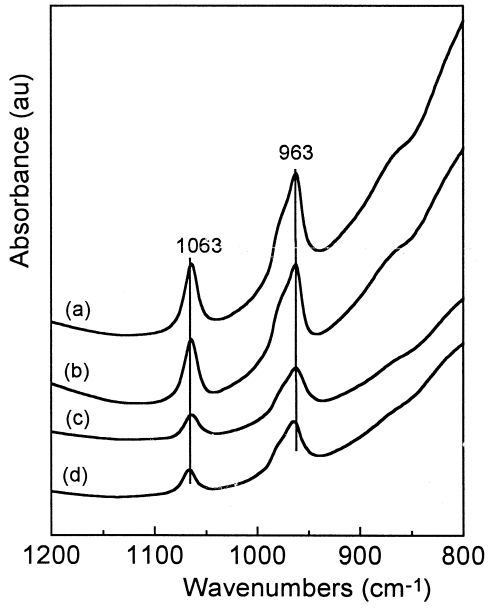

Fig. 2. IR spectra of fresh (a,b) and used (c,d) TiO_2-supported MPMo salt catalysts pretreated at 523 K: (a,c) and (b,d) correspond to NiPMo/T and CoPMo/T, respectively.

Structural changes brought about by catalytic reaction are more clear, specifically for the catalyst pretreated at higher temperatures (Figs. 1B and 2). The spectra of the spent samples previously calcined at 523 K differ only slightly from that of the fresh calcined counterparts. Some increase of the band width and a simultaneous decrease in band intensity becomes apparent, which can be related to some dehydration and/or a certain reduction during on-stream operation [4] (Figs. 1B and 2). A significant

decrease of the Keggin bands takes place on the spent catalyst previously calcined at 623 K (Fig. 1B) with simultaneously appearance of α-MoO_3 band at 993 cm^{-1} which is more discernible compared to that of the fresh one. This can be related to a certain reduction [4] during on-stream operation, i.e., the appearance of a mixture of oxidized and reduced form of 12-molybdophosphoric acid. Finally, the Keggin unit almost completely disappeared in the used catalyst, calcined at 723 K, and the small band of MoO_3 becomes significantly strong.

3.2. Acid properties

Information about the mode of the acid centers on the surface of supported catalysts was previously provided [20] by an IR study of pyridine adsorption. The IR spectra of HPMo/T and Co(Ni)PMo/T catalysts outgassed at different temperatures are presented in Fig. 3. As can be seen pyridine on HPMo/T at 523 K is predominantly adsorbed in a protonated form

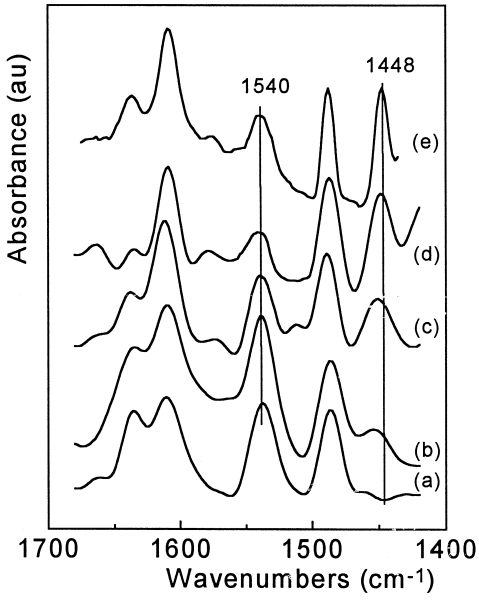

Fig. 3. IR spectra of adsorbed pyridine on the titania-supported heteropolymolybdate catalysts: (a) HPMo/T pretreated at 523 K, (b) HPMo/T pretreated at 623 K, (c) HPMo/T pretreated at 723 K, (d) CoPMo/T pretreated at 523 K, and (e) NiPMo/T pretreated at 523 K.

(Brönsted acidity), visible as a 1540 cm^{-1} band of pyridinium ion. The observed drop in the intensity of this band after outgassing at higher temperatures can be assigned to the lack of protons within the heteropolyanion structure with which a strong interaction can occur. On the one hand, some trapping of the Keggin protons by OH groups of titania can occur with increasing of the temperature, leading to the formation of $TiOH_2^+$ groups. This is similar to the observation for silica-supported heteropoly compounds [23,24]. On the other hand, the loss of acid protons at higher temperatures can be derived from their reaction with the lattice oxygen atoms to produce water [25]. After outgassing at 623 K, a band of Lewis acidity at 1450 cm^{-1} appears, which is related to isolated Mo^{6+} cations of molybdenum oxide phase(s) formed at higher calcination temperature. Both Lewis and Brönsted acidity is observed in CoPMo/T and NiPMo/T samples. The strong band of Lewis acidity in these samples may be assigned to Co^{2+} and Ni^{2+} cations. The increase of Lewis acidity with increasing temperature could be related to the presence of some unsaturated molybdenum ions, $Mo^{\delta+}$ ($6 \leq \delta \leq 4$) [26]. The Brönsted acidity for the supported Co and Ni salts of HPMo can be caused by the incomplete stoichiometry of cation/polyanion and/or some hydrolysis of the molybdophosphate anion during its preparation [6]. It has been proposed [27] that protons can be generated by dissociation of water as a function of electronegativity of the metal cations. Formation of Brönsted acidity in Co(Ni)PMo/T samples (Fig. 3) could result from this phenomenon since water is removed during vacuum heating.

In to measure the catalyst acid strength distribution, the ammonia TPD profiles of HPMo/T catalyst have been recorded and are displayed in Fig. 4A. The broad ammonia desorption peaks indicate the presence of centers of different acid strength. The tendency to decrease the overall acidity with increasing of the temperature pretreatment from 523 to 723 K is accompanied by a shift of the maximum ammonia desorption

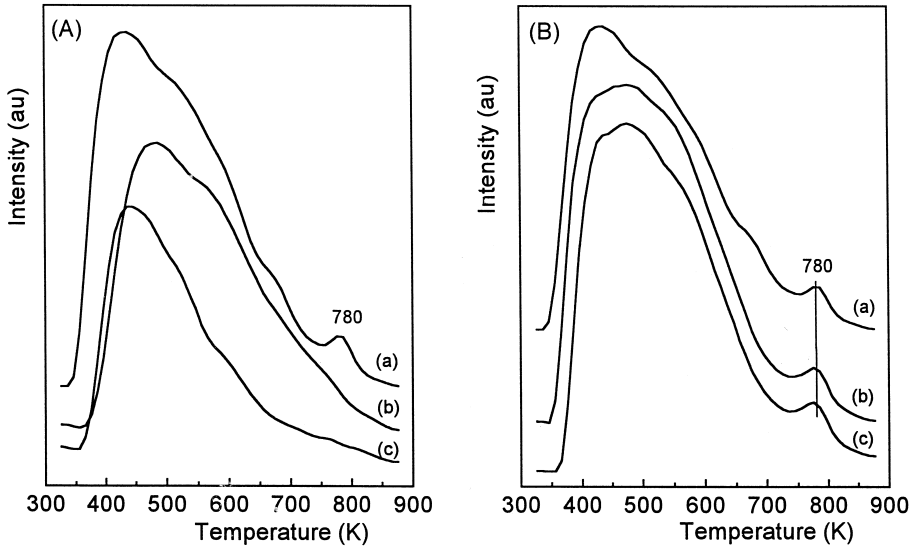

Fig. 4. TPD profiles of adsorbed NH_3 on HPMo/T catalysts (A) subjected to different pretreatment temperatures: (a) 523 K, (b) 623 K, and (c) 723 K; and on MPMo/T salt catalysts pretreated at 523 K (B): (a) HPMo/T, (b) CoPMo/T and (c) NiPMo/T.

peak toward lower desorption temperatures, indicating relatively weaker acid sites. A distinct desorption peak situated at about 750–800 K indicates the presence of strong acid centers that disappear when the sample is pretreated at higher temperatures. The maximum of this peak is close to that of crystalline $HPMo_{12}O_{40}$ [25]. However, this desorption peak is broader than

Table 2
Binding energies (eV) of core electrons of XPMo/T catalysts before and after reaction

Catalysts[a] (pretr)	O1s	$Mo3d_{5/2}$	$Ti2p_{3/2}$	$Ni2p_{3/2}$ ($Co2p_{3/2}$)	P2p
HPMo/T-f (523 K)	530.0 (80) 531.1 (20)	232.1	458.5	–	133.0
HPMo/T-u (523 K)	529.9 (70) 531.0 (30)	231.2 (22) 232.1 (78)	458.5	–	132.7
HPMo/T-f (623 K)	530.0 (83) 531.2 (17)	232.2	458.5	–	133.4
HPMo/T-u (623 K)	529.9 (77) 530.8 (23)	231.1 (20) 232.2 (80)	458.5	–	132.9
HPMo/T-f (723 K)	529.9 (86) 531.1 (14)	232.2	458.5	–	133.7
HPMo/T-u (723 K)	530.0 (81) 531.1 (19)	231.1 (22) 232.2 (78)	458.5	–	133.0
NiPMo/T-f (523 K)	530.0 (82) 531.1 (18)	232.2	458.5	854.6	132.8
NiPMo/T-u (523 K)	529.8 (75) 530.8 (25)	231.1 (26) 232.2 (74)	458.5	854.3	132.8
CoPMo/T-f (523 K)	529.9 (78) 531.2 (22)	232.2	458.5	781.3	132.8
CoPMo/T-u (523 K)	529.9 (77) 531.0 (23)	231.0 (28) 232.2 (72)	458.5	781.0	133.3

[a] f = Fresh; u = Used.

that of the crystalline sample. This indicates a wider distribution of the strong acid sites as a result of the interaction between the HPMo and the TiO_2 carrier.

The TPD profiles of ammonia from NiPMo/T and CoPMo/T after pretreatment at 523 K are presented in Fig. 4B. The relative qualitative difference of these profiles when compared to that of the parent HPMo/T sample at the same temperature, lies in their much more regular desorption profiles. The maxima of ammonia desorption occur approximately at the same temperature ranges, which means that similar strengths are involved, but in the lower temperature range their proportion is higher for Ni(Co)PMo/T samples. The peak at about 780 K also remains in these samples, indicative of the presence of relatively strong acid sites at the surface. The participation of weak acid sites coming from the TiO_2 support would not be ruled out as IR spectra revealed some Lewis acidity on the titania surface (spectra not shown here).

3.3. Surface analysis

Photoelectron spectroscopy has been used to reveal not only the chemical state of the elements but also the changes in concentration brought about by the catalytic reaction. The binding energies (BE) of various core-levels (P2p, $Mo3d_{5/2}$ and $Co2p_{3/2}$ or $Ni2p_{3/2}$) are summarized in Table 2. The XP spectra of the used HPMo/T sample, pretreated at different temperatures, are shown in Fig. 5. The BE of the $Mo3d_{5/2}$ core level for the fresh samples at 232.2 eV is indicative of Mo^{6+} ions (Table 2). However, the spectra of the catalysts subjected to on-stream operation show the overlapping peaks of Mo^{6+} ions and another less intense one at a BE of 231.1 eV associated with a lower oxidation state of Mo (Mo^{5+} ions) [26]. The fraction of reduced molybdenum slightly changes for the used HPMo/T samples with the pretreatment temperature, but it increases for NiPMo/T and CoPMo/T with respect to that of HPMo/T at the same temperature. The results suggest that the surface molybdenum species, involved in the CH_3OH oxidation, include more than one species. The BE for $Ti2p_{3/2}$, $Co2p_{3/2}$ and $Ni2p_{3/2}$ core-levels remain virtually unchanged before and after reac-

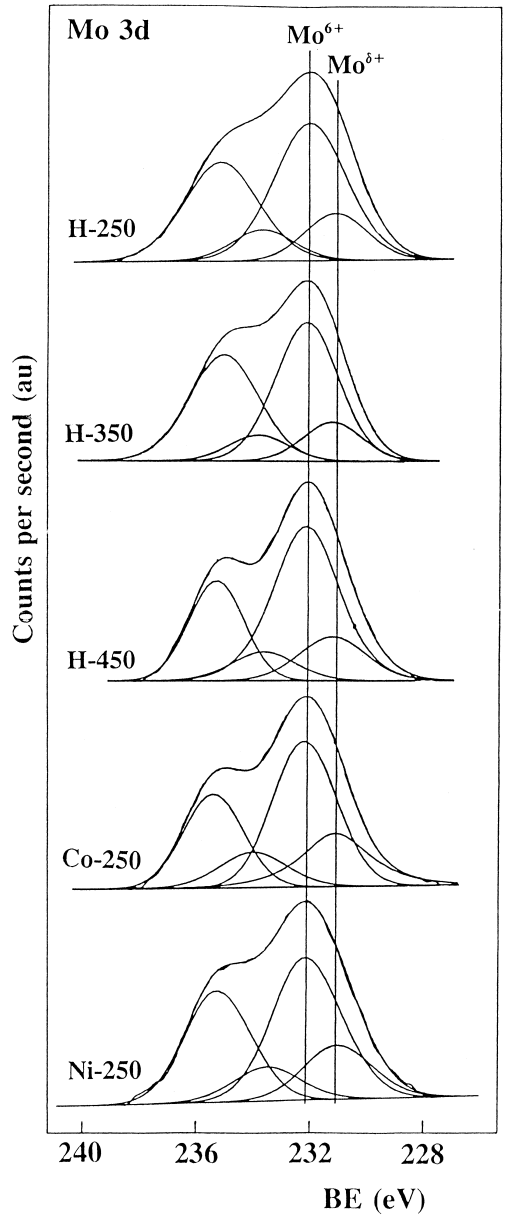

Fig. 5. Mo3d core level spectra of catalysts pretreated at different temperatures and then used in the CH_3OH partial oxidation reaction.

Table 3
Surface atomic ratios of XPMo/T catalysts (subjected to different temperatures of pretreatment) before and after reaction

Catalysts[a]	$(Mo/Ti)_{at}$	$(Ni/Ti)_{at}$ $(Co/Ti)_{at}$	$(P/Ti)_{at}$
HPMo/T-f (523 K)	0.317	–	0.050
HPMo/T-u (523 K)	0.657	–	0.059
HPMo/T-f (623 K)	0.433	–	0.064
HPMo/T-u (623 K)	0.456	–	0.071
HPMo/T-f (723 K)	0.413	–	0.066
HPMo/T-u (723 K)	0.447	–	0.047
NiPMo/T-f (523 K)	0.474	0.077	0.046
NiPMo/T-u (523 K)	0.770	0.143	0.065
CoPMo/T-f (523 K)	0.375	0.067	0.045
CoPMo/T-u (523 K)	0.579	0.070	0.077

[a] f = Fresh; u = Used.

tion (Table 2) and correspond to Ti^{4+}, Co^{2+} and Ni^{2+} ions, respectively. However, the BE of P2p for the used HPMo/T catalyst decreases with respect to its fresh counterpart (Table 2), suggesting that the chemical environment of the phosphorus changes under reaction conditions. The O1s peak displays two components with binding energies of 529.9 and 531.0 eV (Table 2): the former is related to oxo-molybdenum species, while the latter is probably due to the OH groups on titania. This assignment is supported by the fact that the electron density in the OH group is substantially lower than in the lattice oxygen, and also because the intensity of the component at ca. 531.0 eV decreases with increasing of the pretreatment temperature.

From the peak intensities and atomic sensitivity factors, surface (XPS) atomic ratios have been computed [28]. Variations of the XPS Mo/Ti atomic ratios of the catalysts, subjected to different pretreatment temperatures before and after reaction are listed in Table 3. The values of XPS Mo/Ti ratios of the used catalysts are higher than those of the fresh ones. The XPS ratio for HPMo/T at 523 K is the highest, indicating that the exposure of HPMo is preserved during reaction. In addition, the higher XPS Mo/Ti ratios than the Mo/Ti ratios derived from chemical analysis (Table 1) suggest that the components are well dispersed on the support surface. The XPS Mo/Ti ratio decreases with increasing of the temperature (Table 3). A similar tendency is observed for the fresh catalysts, indicating that breaking of the large oxo-anions into smaller structures yields well dispersed molybdenum oxide phases at 623 K. However, at higher pretreatment temperatures there is some aggregation, caused by the formation of bulk MoO_3, as already revealed by IR spectra. Therefore, it appears that thermal decomposition of the HPA into MoO_3 undergoes some rearrangement of the heteropoly anion forming an intermediate oxide compound with preserved Keggin unit although the molybdenum ions are placed in a distorted octahedral environment of oxide ions. This transformation of HPA is favored during the methanol oxidation reaction due to some reduction of molybdenum species.

3.4. Redox properties

The redox properties of the catalysts have been revealed by TPR in a hydrogen flow. The TPR profiles of the samples (Fig. 6) display a single TPR peak with a maximum at 789, 762

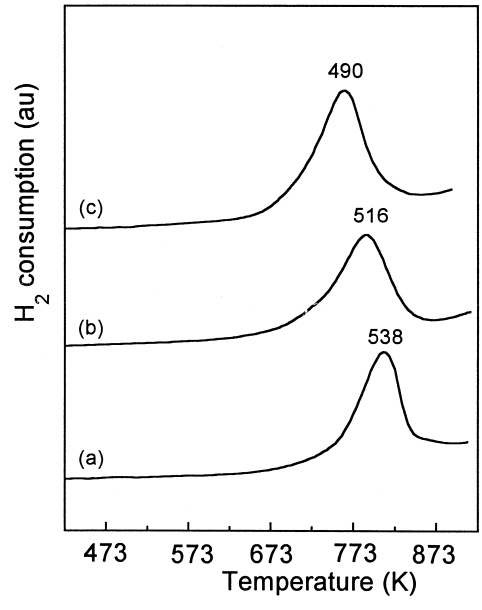

Fig. 6. TPR profiles of TiO_2-supported molybdophosphate catalysts: (a) CoPMo/T, (b) HPMo/T, and (c) NiPMo/T.

Table 4
Methanol oxidation over titania-supported 12-molybdophosphates subjected to different calcination temperatures at $T_{reac.} = 503$ K

Sample (pretr)	Conversion (%)	Yields (%)			
		CH_3OCH_3	HCHO	$HCOOCH_3$	CO_2
HPMo/T (523 K)	27.4 (18.5)	11.7 (12.4)	10.0 (3.6)	5.6	0.1
HPMo/T (623 K)	15.6 (5.0)	3.2 (2.1)	8.6 (2.9)	3.7	0.2
HPMo/T (723 K)	14.2 (6.0)	3.0 (2.2)	7.7 (3.8)	3.3	0.3
NiPMo/T (523 K)	12.0 (4.4)	2.0 (1.7)	5.7 (2.7)	4.3	–
CoPMo/T (523 K)	13.5 (5.5)	3.2 (2.4)	7.9 (3.1)	2.4	0.1

Values in parenthesis are data obtained at 483 K.

and 811 K for catalysts HPMo/T, NiPMo/T and CoPMo/T, respectively. The reduction temperature maximum of the samples can be attributed to the reduction of octahedrally coordinated Mo^{6+} of polymolybdates to a lower valence state (Mo^{5+} and/or Mo^{4+}) [29]. The highest hydrogen consumption is observed for NiPMo/T, probably as a consequence of the hydrogen spillover produced by the reduced nickel. The comparison of HPMo/T and CoPMo/T catalysts reveals not only that the former is reduced at somewhat lower temperature than the latter, but also a higher H_2 consumption in catalyst HPMo/T. This means that the molybdenum in catalyst HPMo/T is easily reduced than in CoPMo/T sample.

3.5. Catalyst performance

The effect of temperature pretreatment on the catalytic behaviour of the samples was investigated. The methanol conversion and the yields of different products at reaction temperatures of 483 and 503 K are presented in Table 4. The catalytic behaviour data of the samples at 503 K are taken from Ref. [20]. The main products

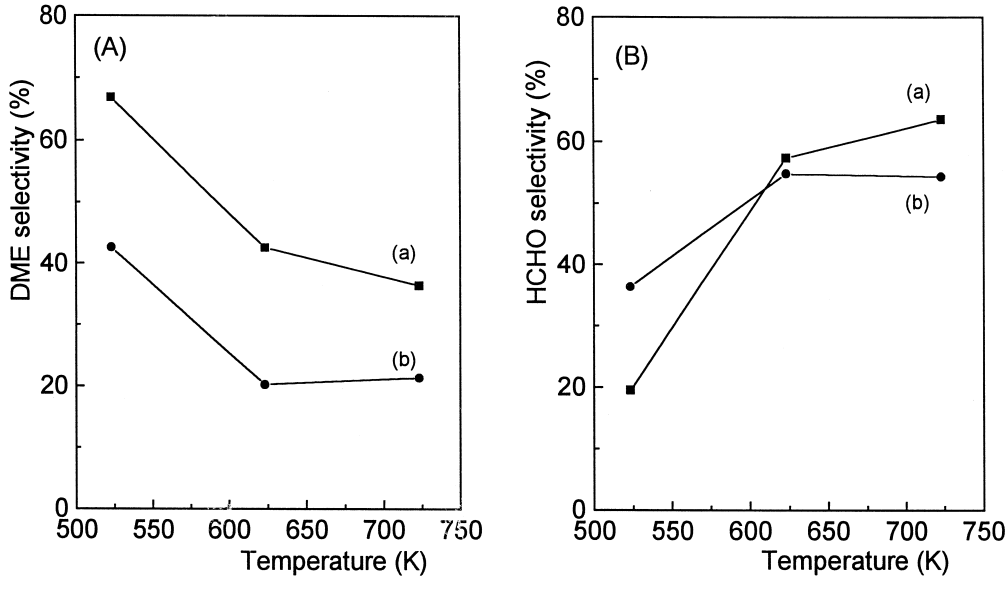

Fig. 7. Dependence of DME (A) and HCHO (B) selectivity of HPMo/T catalyst on pretreatment temperature at reaction temperatures of (a) 483 K, and (b) 503 K.

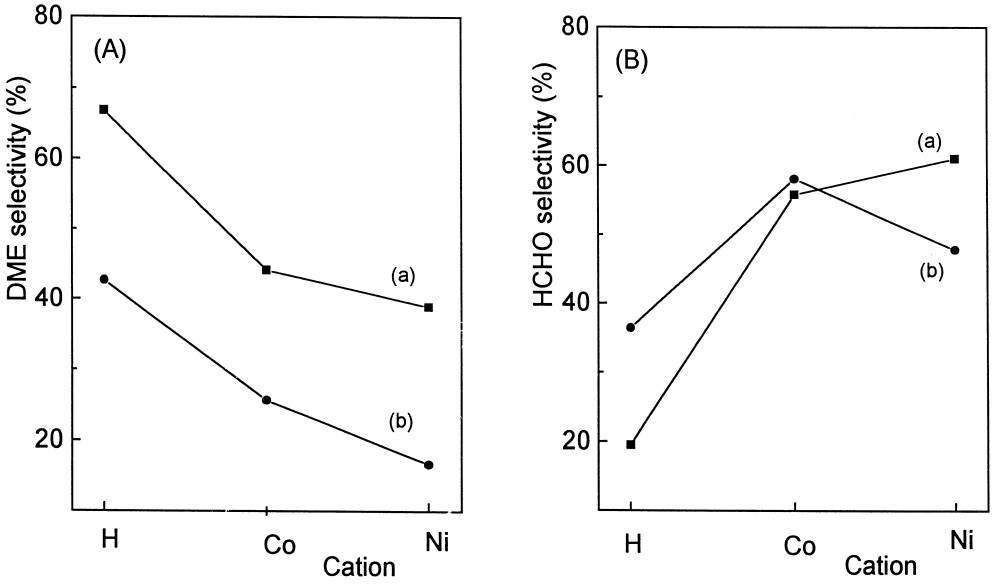

Fig. 8. Dependence of DME (A) and HCHO (B) selectivity of TiO_2-supported molybdophosphate catalysts on the cation at reaction temperatures of (a) 483 K, and (b) 503 K.

observed from methanol oxidation are dimethyl ether (CH_3OCH_3, DME), formaldehyde (HCHO) and methyl formate ($HOOCCH_3$). Some traces of CO_2 are observed at higher reaction temperature. Changes in the selectivity to DME and HCHO selectivity over titania-supported HPMo catalyst as a function of the pretreatment temperature are shown in Fig. 7. The

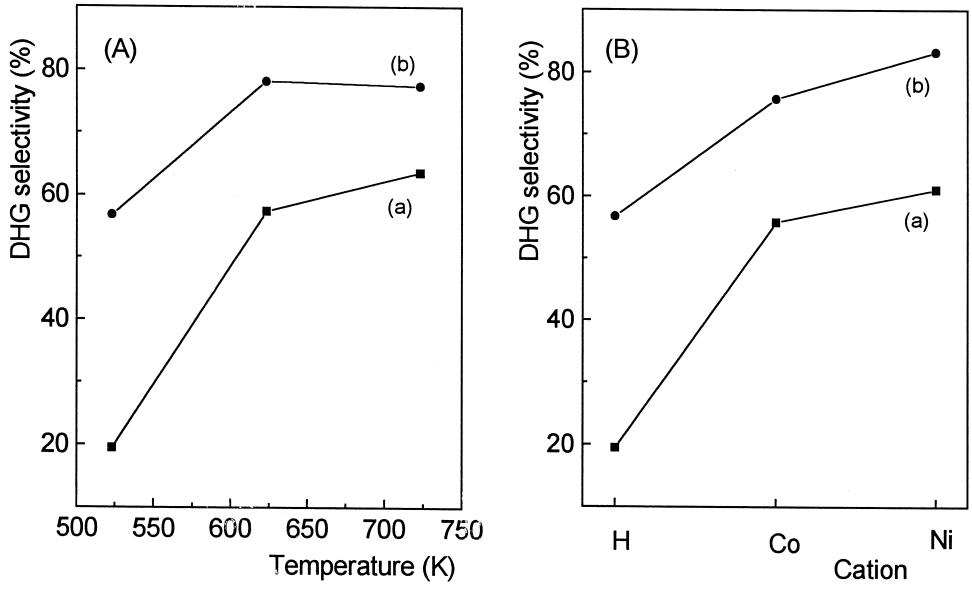

Fig. 9. Dependence of the dehydrogenation selectivity (DHG) of HPMo/T on the pretreatment temperature (A) and on the cation (B) at reaction temperatures of (a) 483 K, and (b) 503 K.

HPMo/T sample calcined at 523 K exhibits the highest DME selectivity and yield as well as the largest methanol conversion (Table 4). After increasing of the temperature from 523 to 623 K for the HPMo/T, a significant decrease of both the selectivity and the yield of CH_3OCH_3 are observed (Fig. 7A and Table 4). However, increasing the temperature up to 623 K leads to a significant increase in HCHO selectivity (Fig. 7B). A further increase of pretreatment temperature up to 723 K does not produce great changes in the catalytic performance. The dependence of the DME and HCHO selectivity on the change of the protons in the HPMo acid by Co and Ni cations is shown in Fig. 8. Replacement of the protons by Co and Ni leads to a decreased DME selectivity and an increased dehydrogenation selectivity. Dehydrogenation selectivity of HPMo/T and Ni(Co)PMo/T, presented as a sum of the mild oxidation products (HCHO + CO_2) [10], is shown in Fig. 9. The dehydrogenation selectivity, which increases for all the samples with increasing of the calcination temperature, is always higher at a reaction temperature of 503 K.

4. Discussion

4.1. Structural features and thermal stability

In our previous work [19], it has been shown that the thermal decomposition of the supported HPMo proceeds in two steps: (i) gradual dehydration of the heteropoly compound with formation of anhydrous phase, the Keggin unit being preserved, and (ii) transformation of heteropoly anion into molybdenum oxides with different morphological phases and phosphates, which is completed at temperature above 773 K. A similar characterization has been carried out on the used samples in order to know if the catalysts remain unchanged or not during the catalytic reaction for a given pretreatment temperature. This may provide an explanation for the marked influence of the pretreatment conditions on the catalytic behavior of these catalysts in CH_3OH oxidation.

The present IR results provide clear evidence on the preservation of the Keggin unit up to 623 K pretreatment after test reaction, as revealed by the XPS Mo/Ti ratio (Table 3), although with some partial decomposition. This fact is not surprising, because under the conditions of methanol oxidation 'heteropolymolybdate blue' [30] could be formed, and also there is water vapor in the catalyst environment. These two factors are known to increase the stability of HPMo with a Keggin structure. These mixed-valence compounds contain Mo^{6+} and Mo^{5+} formed by the rapid electron trapping among the 12 equivalent Mo atoms in a Keggin anion and the anion structure is maintained [31–33]. The presence of the MoO_3 band only in the IR spectra of the used HPMo/T pretreated at 723 K indicates that in the conditions of the CH_3OH oxidation reaction the HPMo is almost destroyed at temperature lower than that of the fresh catalyst. Rocchiccioli-Deltcheff et al. [11] have also reported that after different thermal treatments from 523 to 773 K, the silica-supported 12-HPMo catalysts exhibit very poor infrared spectra after catalytic reaction. However, the authors showed that silica support decreases the thermal stability of supported HPMo and the transformation into β-MoO_3 begins at a temperature lower than that of the bulk. Taking this into consideration, a lower stability of the silica-supported HPMo should be expected under reaction conditions compared to titania-supported HPMo. It has been concluded [19] that the stability of the HPMo supported on titania increases due to the titania-support interaction.

The most important affect on Mo dispersion occurs after catalyst pretreatment at 523 K, at which a significant increase of the XPS Mo/Ti ratios (Table 3) is observed. Probably, the preliminary clusters of heteropolymolybdate anions are broken into smaller oxoanions with a preserved Keggin unit which remain well dispersed even after prolonged on-stream operation. The

dispersion of molybdenum species after reaction is less affected for samples at higher pretreatment temperatures, probably, because of the presence of thermally more stable β- and/or α-MoO_3 phases [19].

4.2. Acidity

The IR data of pyridine adsorption and the ammonia TPD experiments consider that the acidic centers in the titania-supported HPMo are of Brönsted (protonic) and Lewis type and the acidic properties of the samples depend on their hydration degree. According to literature data [25,30] two types of protons: nonlocalized hydrated protons, and nonhydrated, less mobile protons has been distinguished. It should be noted, that most of the constitutional protons present weak acid centers, rather firmly bound to the Keggin anion, whose amount decreases upon thermal treatment. It has been shown [34] that silica-supported HPMo calcined at 323 K only absorbed 1.5 pyridine molecules per Keggin anion. The amount absorbed by the same sample pretreated at 623 K was half this value and only 25% of the constitutional protons were contributed to the strong acidity of the samples.

The large ammonia desorption peak in the lower temperature range of the spectra (Fig. 4) can be assigned to acidic sites of weak and/or moderate strength due to the presence of constitutional protons as well as of Lewis acid sites, caused from the positively charged cations (Mo^{6+} and/or Co^{2+} and Ni^{2+}). However, the higher temperature peak revealed in the spectra of the samples pretreated at 523 K (Fig. 4) shows the presence of strong acid sites, which could be mainly associated with some hydrated protons retained by the bulk of the acid phase, which disappear with increasing of the temperature pretreatment. As can be seen from ammonia desorption profiles of the HPMo/T sample pretreated at 523 and 723 K (Fig. 4A), the dehydration process reduces both, the number of the acidic centers able to absorb NH_3 and their strength causing shift towards relatively weaker sites. The sample which is pretreated at a lower temperature and therefore retained more constitutional protons contains a significant amount of acidic centers, whereas the sample pretreated at a higher temperature lack such acidic sites and the Lewis type sites should be dominant, being seen from IR (Fig. 3).

4.3. Activity

According to the mechanism of the methanol dehydration on the oxide catalysts based on an overview of many data [35–38], the main step consists of a formation of the methoxy intermadiate on the acid sites of the catalyst. This intermediate can either, react with another methanol molecule to form dimethyl ether (acid-base pathway), or undergo a nucleophilic attack of surface oxide ion to form a precursor of formaldehyde (redox pathway). Therefore, it could be expected that the different structures present on the surface of the catalysts [19] would influence in a different way the various elementary steps of the transformation of methanol and hence the selectivity of the reaction.

The highest selectivity to DME at 523 K (about 70%) (Fig. 7A) suggests that the undecomposed HPMo acid on the titania surface behaves as an acid catalyst, containing protons available to protonate methanol [35,38]. Pretreatment of the catalyst at a higher temperature suppresses the Brönsted acidity, being seen from the Fig. 3. The latter leads to an increase of the redox selectivity, HCHO formation, (Fig. 7B) at the expense of CH_3OCH_3 (Fig. 7A). Replacement of the protons in HPMo acid by cations (Ni and Co) also causes a substantial change of the proton donor capacity of the acid centers and hence the selectivity to DME decreases compared to that of supported HPMo (Fig. 8A). The role of acidic protons in a dehydration reaction has been investigated by many authors [39–41] and has been found that the overall methanol oxidation rate on HPVMo/KPMo catalysts depends on the number of protons per

Keggin unit. The lack of protons decreases the concentration of protonated methanol and the amount of the common intermediate between DME and dehydrogenation products [40], which lead to a decreased conversion (Table 4).

The lower DME selectivity for the NiPMo/T sample compared to that of CoPMo/T (Fig. 8A) would be an indication of a higher degree of substitution of protons with Ni atoms. On the other hand, NiPMo/T and CoPMo/T show a significant selectivity to DME (Fig. 8A), due to the acidic protons, as revealed by TPD of NH_3 and IR of pyridine. The formation of protonic acidity during the reaction is also possible as a result of the exposure of the salts to water vapor, produced during methanol transformation, and its dissociation on the metal cations [27]. Since for dehydration of methanol moderate and strong acid sites are required [41], it may be assumed that the cation substituted samples contain, besides strong acid sites, a large distribution of weak and moderate acid strength (Fig. 4b,c), sufficient to protonate methanol. However, the catalytic properties of Co(Ni)-PMo/T catalysts do not correlate with the bulk acidity of these samples. The selectivity to DME should vary with the proton content, which is not the case, the HPMo/T sample is more active than Co(Ni)PMo/T samples. Ammonia, as a polar molecule, can enter into the whole crystallites and neutralize all the bulk protons. Probably, NiPMo/T and CoPMo/T contain superficial sites of moderate strength which contribute to the high activity in methanol dehydration. This is supported by the higher values of the surface area and XPS Mo/Ti atomic ratio of these samples (Tables 1 and 3).

The catalysts have a complex composition in the temperature range of 623–723 K [19]: (i) not yet totally destroyed HPA with preserved Keggin unit and (ii) the presence of β- and α-MoO_3 phases, the latter dominates at higher temperature (723 K). Therefore, in the region corresponding to the appearance of the anhydride phase and molybdenum oxide phases with different morphological composition, the concentration of the constitutional protons is insignificant and the selectivity to DME begins to decrease with parallel increase of the selectivity to HCHO (Fig. 7). The increase of the HCHO formation with increasing of the temperature pretreatment has been explained on the basis of a mechanism which requires the presence of two adjacent surface dioxo units existing on the (010) surface of a well dispersed MoO_3, whereas MoO_3 (100) leads to a methyl formate formation (46,47). Therefore, the observed increase in the redox properties of the catalysts with the temperature (Fig. 7) is caused mainly from the transformation of HPMo into molybdenum oxide phases.

The TPR and XPS results suggest that the surface Mo in supported catalysts tend to be slightly reduced during methanol oxidation reaction. Variation of the intensity of the IR bands of the used catalysts with increasing of the pretreatment temperature (Fig. 1BFig. 2B) also consists with the presence of reduced molybdenum sites under reaction conditions. Consequently, the presence of both, the bulk MoO_3 produced during on-stream, as observed by IR (Fig. 1), and the reduced molybdenum sites would retard the production of HCHO; approximately the same selectivity to HCHO after pretreatment at 623 and 723 K is observed (Fig. 7B). However, the presence of oxygen in the gas phase maintains the high oxidation state of the surface molybdenum atoms, inhibiting their deep reduction. Reoxidation of the reduced molybdenum by gaseous oxygen would be occurred during reaction conditions. The latter can be confirmed by the constancy of the XPS Mo/Ti ratio and of the fraction of reduced molybdenum (Tables 2 and 3). Consequently, the higher selectivity to HCHO in the temperature range of 623–723 K is maintained by the higher electron density of the molybdenum bridging oxygen atoms according to the mechanism of HCHO formation [37,42].

The reducibility trends derived from TPR experiments do not correlate with methanol activity. Since the catalytic reactivity is only con-

trolled by the surface reduction process, the contribution of the bulk reduction may result negligible for this study. The T_{max} temperature presented in Fig. 6 reflects the ease of reduction by oxygen removal from the catalyst. However, the difference in the selectivity to HCHO at reaction temperatures of 483 and 503 K may originate from the difference in the amount of reduced molybdenum. Less reduced molybdenum species would increase the number of molybdenum bridging oxygen sites, which can activate the formation of HCHO. As can be seen in Fig. 9, there is a difference among the catalysts with respect to the change of their dehydrogenation selectivity at both reaction temperatures. According to Ref. [43], the formation of methylformate on supported-molybdenum catalysts requires the presence of both, isolated oxo-molybdenum sites and methoxy groups on the support, which can be formed from the interaction of methanol with hydroxyl groups of titania. It should be noted that the participation of the titania surface in the reaction can not be excluded. Possibly, the adsorbed formaldehyde species spillover onto the titania surface, react with methoxy groups and form a hemiacetal intermediate [43] which is transformed into methylformate. From the XPS data, it is seen that the concentration of Ti–OH groups increases in the used catalysts (especially for NiPMo/T) (Table 2). This means that the free titania surface could induce an increased methoxy group concentration and hence the formation of methylformate at the expense of HCHO formation. This phenomenon is clearly visible in the case of the NiPMo/T sample: a lower HCHO selectivity (Fig. 8B) corresponds to a higher $HCOOCH_3$ formation, which leads to an increased dehydrogenation selectivity (Fig. 9).

The present study illustrates how the selectivities in methanol oxidation can be tailored by appropriate catalyst pretreatment which define the specific surface architectures of titania-supported 12-molybdophosphates which are responsible for these reactions.

Acknowledgements

S.D. thanks the Ministerio de Educacion y Cultura for a NATO grant. The authors would like to thank Dr. M. Lopez Granados for helping in the ammonia TPD measurements. Financial support from CICYT, Spain, under project MAT95-0894 is also acknowledged.

References

[1] C.L. Hill, C.M. Posser-McCarthy, Coord. Chem. Rev. 143 (1995) 407.
[2] N. Mizuno, M. Misono, Chem. Rev. 98 (1998) 198.
[3] M.T. Pope, Heteropoly and Isopoly Oxometalates, Springer-Verlag, Berlin, 1983.
[4] M.H. Dickman, M.T. Pope, Chem. Rev. 94 (1994) 569.
[5] D.C. Dunkan, R.C. Chambers, E. Hecht, C.I. Hill, J. Am. Chem. Soc. 117 (1994) 681.
[6] I.V. Kozhevnikov, Chem. Rev. 98 (1998) 171.
[7] J.C. Edwards, C.Y. Thiel, B. Benac, J.F. Knifton, Catal. Lett. 51 (1998) 77.
[8] C. Rocchioccioli-Deltcheff, A. Aouissi, M. Bettahar, S. Launay, M. Fournier, J. Catal. 164 (1996) 16.
[9] A. Jürgensen, J.B. Moffat, Cat. Lett. 34 (1995) 237.
[10] J.M. Tatibouët, C. Montalescot, K. Brückman, J. Haber, M. Che, J. Catal. 169 (1997) 22.
[11] C. Rocchioccioli-Deltcheff, A. Aouissi, S. Launay, M. Fournier, J. Mol. Catal. A: Chem. 114 (1996) 331.
[12] C. Nowinska, R. Fiedorow, J. Adamiec, J. Chem. Soc., Faraday Trans. 87 (1991) 749.
[13] Y. Izumi, K. Urabe, Chem. Lett. 663 (1981) .
[14] M. Schwegler, P. Vinke, M. van Bekkum, Appl. Catal. A 80 (1992) 41.
[15] S. Kasztelan, E. Payen, J.B. Moffat, J. Catal. 112 (1988) 320.
[16] C. Rocchiccioli-Deltcheff, M. Amirouche, G. Harve, M. Fournier, M. Che, J.M. Tatibouët, J. Catal. 126 (1990) 591.
[17] R. Fricke, G. Öhlman, J. Chem. Soc., Faraday Trans. I 82 (1986) 263.
[18] W.C. Cheng, P. Luthra, J. Catal. 109 (1988) 163.
[19] S. Damyanova, J.L.G. Fierro, Chem. Mater. 10 (1998) 871.
[20] M.L. Cubeiro, S. Damyanova, J.L.G. Fierro, Catal. Lett. 49 (1997) 223.
[21] G.A. Tsigdinos, Ind. Eng. Chem., Prod. Res. Dev. 13 (1974) 267.
[22] C. Rocchiccioli-Deltcheff, K. Thouvenot, R. Franck, Spectrochim. Acta, Part A 32 (1976) 587.
[23] C. Rocchiccioli-Deltcheff, M. Amirouche, M. Fournier, J. Catal. 138 (1992) 445.
[24] R. Thouvenot, C. Rocchiccioli-Deltcheff, M. Fournier, J. Chem. Soc., Chem. Commun. 1352 (1991) .
[25] B.K. Hodnett, J.B. Moffat, J. Catal. 88 (1984) 253.
[26] S. Damyanova, J.L.G. Fierro, Appl. Catal. A: Gen. 144 (1996) 59.
[27] H. Niiyama, Y. Saito, E. Echigoya, Proc. 7th Int. Congr. Catal., 1980, p. 1416.

[28] D. Briggs, M.P. Seah, Practical Surface Analysis, Auger and X-ray Photoelectron Spectroscopy, 2nd edn. Wiley, Chichester, 1990.
[29] S. Damyanova, A. Spojakina, K. Jiratova, Appl. Catal. A: Gen. 125 (1995) 257.
[30] D.C. Duncan, C.L. Hill, Inorg. Chem. 35 (1996) 5828.
[31] C. Sanchez, J. Livage, J.P. Launay, M. Fournier, Y. Yeannin, J. Am. Chem. Soc. 104 (1982) 3194.
[32] K. Eguchi, Y. Toyozawa, N. Yamazoe, T. Seiyama, J. Catal. 83 (1983) 32.
[33] G.M. Brown, M.-R. Noe-Spirlet, W.R. Busing, H.A. Levy, Acta Crystall. B 33 (1987) 1038.
[34] E.A. Paukshtis, O.I. Goncharova, T.M. Yureva, E.N. Yurchenko, Kinet. Katal. 27 (1986) 463.
[35] J.G. Highfield, J.B. Moffat, J. Catal. 95 (1985) 108.
[36] K. Brückman, J.M. Tatibouët, M. Che, E. Serwicka, J. Haber, J. Catal. 139 (1993) 455.
[37] R.S. Weber, J. Phys. Chem. 98 (1994) 2999.
[38] J.M. Tatibouët, Appl. Catal. A: Gen. 148 (1997) 213.
[39] J.G. Highfield, J.B. Moffat, J. Catal. 89 (1984) 185.
[40] E.M. Serwicka, E. Broclawik, K. Brückman, J. Haber, Catal. Lett. 2 (1989) 351.
[41] N. Essayem, G. Coudurier, M. Fournier, J.C. Vedrine, Catal. Lett. 34 (1995) 223.
[42] I.V. Kozhevnikov, A. Sinnema, J.J. Jansen, H. van Bekkum, Catal. Lett. 27 (1994) 187.
[43] C. Louis, J.M. Tatibouët, M. Che, J. Catal. 109 (1988) 354.